Ion mobility mass spectrometry of in situ generated biomass pyrolysis products

Clément Castilla, Christopher Rüger, Hélène Lavanant, Carlos Afonso

Ion mobility mass spectrometry of *in situ* generated biomass pyrolysis products

Clément Castilla[1], Christopher P. Rüger[1,2,3], Hélène Lavanant[1], Carlos Afonso[1,3]

1. *Normandie Univ, UNIROUEN, INSA Rouen, CNRS, COBRA, 76000 Rouen, France*
2. *Universitat Rostock, Institut für Chemie, Abteilung für Analytische und Technische Chemie, Dr.-Lorenz.-Weg 2, Rostock, DE 18059*
3. *International Joint Laboratory – iC2MC: Complex Matrices Molecular Characterization, TRTG, BP 27, 76700 Harfleur, France*

Abstract

Lignocellulosic biomass is an abundant and renewable energy source that can be used as biofuel after physicochemical conversion, e.g. by fast pyrolysis. However, the chemical variations from wood and other biomass species affect this conversion. Chemical characterization is needed to obtain more information on the pyrolysis products depending on the biomass type and pyrolysis conditions. Here, we compared the fast pyrolysis molecular pattern of five lignocellulosic biomasses (beech, hickory, miscanthus and two brands of resinous wood pellets) obtained from a direct analysis method of solid samples coupled to ion mobility and time of flight mass spectrometry (IM-TOF MS). Fourier transform ion cyclotron resonance mass spectrometry (FTICR MS) with its ultra-high resolving power was used, with a similar solid analysis introduction approach, to probe for the presence of possible unresolved isobaric compounds in the IM-TOF MS analysis. Isobaric interferences were found to be negligible and molecular formulas determined using IM-TOF MS were confirmed as reliable. Principal component analysis on the molecular formulas allowed the extraction of marker ions preferentially found in hardwood and miscanthus or softwood species. Ion mobility drift time values from these biomass markers were converted into collision-cross sections (CCS), a direct measure of structure and shape of a molecule. No significant CCS differences were observed between the markers of the five wood samples, showing isomeric similarities between the samples. In order to move forward on the structural elucidation and characterization of the pyrolysis products, IM-TOF MS and tandem mass spectrometry (MS/MS) were performed on standard molecules and compared to the biomass pyrolysis products, highlighting the presence of isomers in the wood pyrolysis products.

Highlights

- **Five pelletized lignocellulosic biomass samples in atmospheric solid analysis probe**
- **Ion mobility mass spectrometry for fast isobaric and isomeric fingerprinting**
- **Differentiation with principal component analysis on molecular formulas**
- **Tandem mass spectrometry coupled to ion mobility evidenced the presence of isomers**
- **Collision cross section determination and comparison**

Keywords: Ambient ionization, lignocellulosic biomass, ion mobility, ultra high resolution mass spectrometry, biomass pellets, multivariate data analysis

1. Introduction

Lignocellulosic biomass is an abundant and renewable energy source that can be used as an alternative to fossil fuel, directly for heating purposes or as biofuel after physicochemical conversion. The usage of biomass or biomass-derived fuel for power generation is steadily increasing [1], motivated by its low carbon footprint [2]. Biomass includes agricultural waste, aquatic plants or algae, wood, and wood waste. Wood is mainly composed of cellulose, hemicellulose, lignin and extractable compounds [3, 4]. Cellulose and hemicellulose are polymers constituted of sugar units. Lignin is a complex reticulated polymer based on p-coumaryl (H unit), coniferyl (G unit) and sinapyl (S unit) building blocks. Wood composition can differ according to the species [5]. Softwood (*gymnosperm*) and hardwood (*angiosperm*) are the two dominant wood families. Softwood and hardwood can be differentiated by the proportion of the lignin monomeric units and the molecular profile of their extractable compounds. Hardwood lignin contains equivalent proportion of G and S units with traces of H units, whereas softwood lignin mainly contains G units with few H units [6]. The chemical differences from wood and other biomass species affect the conversion of biomass to biofuel. Conversion of wood for energy purposes can be done by pyrolysis and results in gas, solid and liquid products [7-9]. These products will have different chemical properties depending on the pyrolysis parameters *e.g.*, fast or slow pyrolysis [10]. Chemical characterization is needed to obtain more information on the pyrolysis products depending on the biomass and pyrolysis process used.

In the last decades, several analytical methods have been developed for the description of solid biomass, among which pyrolysis mass spectrometry (Py-MS) is frequently used [11]. In Py-MS, the solid biomass is decomposed in a pyrolizer unit, and the evolved gas mixture is subjected to gas chromatographic separation or directly to mass spectrometric detection. Curie point filament and direct insertion probe (DIP) are two pyrolyzing approaches used for Py-MS. In a Curie point pyrolizer, the sample is coated on a filament submitted to fast inductive heating. With the direct insertion probe, the sample is inserted into an inert support and pyrolyzed by resistive heating. The pyrolysis products obtained are ionized, in most cases, under vacuum pressure using electron ionization (EI). These techniques have been applied to wood pyrolysis compounds in several studies [12-15]. Coupling gas chromatography to Py-MS (Py-GC-MS) allows a supplementary separation dimension, particularly useful for targeted approaches and structural elucidation [12, 14, 16, 17]. Gas chromatography, and in particular GC x GC remains, to this day, the gold standard in isomeric separation [18] but one analysis can last several minutes or hours. Pyrolysis gas chromatography suffers from similar drawbacks and limitations as conventional gas chromatography: the analytes have to pass the separation column by means of volatility and stability. Certain polar constituents are difficult to detect by GC-MS. The presence oxygen in molecules lower vapor pressure by an order of magnitude or more compared to hydrocarbons, consequently limiting their analysis by GC-MS. Moreover, polar functionalities, such as carbonyls, are prone to decompose during long gas chromatographic analyses and molecules with high boiling points tend to remain trapped within the system. In addition, the use of a vacuum ionization source such as EI involves extensive fragmentation, making the interpretation of spectra from complex mixtures more challenging.

The development of ambient ionization methods operating at atmospheric pressure —where soft ionization occurs, giving low source fragmentation— led to new methods for direct analysis of solid samples. Atmospheric solid analysis probe (ASAP) or direct insertion probe (DIP) with atmospheric pressure chemical ionization (APCI) are two systems adapted to the analysis of solid or high viscous materials. With the ASAP source developed by McEwen *et al.* [19], the solid sample, contained in a glass capillary, is evaporated by a hot nitrogen gas stream, subsequently ionized within a nitrogen

plasma. Fast analysis is feasible and minimal fragmentation is achieved by DIP or ASAP for small molecules, whereas larger molecules such as polymers lead to the formation of pyrolysis products [20]. Using this technique, biomass pyrolysis products have been described in a few studies [21, 22]. DIP is similar to ASAP except for geometric aspects regarding the source design and dimensions [23]. The immediate transfer and ionization in the heated ion source of the freshly pyrolyzed species should overcome the volatility and transfer limitations of gas chromatography and highly-polar species can be detected.

Differentiation of isobaric compounds found in complex matrices such as biomass pyrolysis products requires high resolving power. In that respect, Fourier transform ion cyclotron resonance mass spectrometer (FTICR MS) can be used with DIP APCI. FTICR MS provides high resolving power and mass accuracy, allowing separation of isobaric species. FTICR MS was used for many applications such as biomass [24], bio-oil [25] and aerosols [26] analyses. However, molecular formulas obtained with FTICR MS give only limited structural information as a molecular formula can correspond to many isomers. In that respect, ion mobility spectrometry mass spectrometry (IMS-MS), can be used as a complemental technique. In IMS, ions traverse a gas-filled ion mobility cell guided by an electric field and are separated by their size, shape and charge that gives rise to different drift time values [27]. This technique allows the separation of isomers and was used in numerous studies [28, 29]. The drift times (t_D) from the ions observed with IMS can be converted to experimental collision cross sections (CCS). CCS is a molecular descriptor that depends on the buffer gas used (generally N_2 or He) and is linked to the ion size and shape. Ion mobility and ion mobility mass spectrometry were used in few studies for the identification of wood species [30, 31]. In the study of Lawrence *et al*. and Pettersen *et al.*, the global ion mobility profile was used to compare volatiles compounds from different wood samples. Moreover, the identification of several volatile compounds was achieved, and GC-MS experiments were used to support IMS data. However, at present, no study involving ion mobility directly coupled with mass spectrometry exists on wood pyrolysis products and no CCS were determined for these pyrolysis products.

This study builds upon a previous study which was based on the development of a DIP FTICR MS method for the characterization and differentiation of hardwood samples [32]. Using DIP, we aimed for the chemical description and differentiation of fast pyrolysis products of biomass by direct evolved gas analysis (EGA) approaches. Comprehensive chemical description deploying direct EGA techniques requires ultra-high resolution mass spectrometric detection. Nonetheless, ultra-high resolution provides information on molecular formulas but with no structural elucidation. The addition of ion mobility spectrometry allows to retrieve additional information on the isomeric content, without any significant increase of experiment time. In this study, ASAP was used with ion mobility and time of flight mass spectrometry (IM-TOF MS) to compare pyrolysis products from hardwood, softwood and miscanthus samples. The possible presence of unresolved isobaric compounds was investigated using DIP and the ultra-high resolving power of FTICR MS. Principal component analysis allowed the extraction of molecular markers relative to hardwood of softwood samples, and collision cross sections in nitrogen (CCS_{N2}) were determined for these markers using ion mobility. Also, the CCS_{N2} of standard molecules were determined and compared to the CCS_{N2} from biomass pyrolysis products. Further structural analysis was performed by comparison of MS/MS spectra from wood degradation markers and standard molecules to reveal the presence of isomers.

2. Materials and methods

2.1. Samples

Five different wood pellet types were investigated for this study. Two pellet types are representatives of hardwood: beech (Ooni, Edinburgh, Scotland) and hickory (Traeger Pellet Grills, Salt Lake City, USA). Two pellet types are representatives of softwood species: two brands of resinous wood pellets (Crepito®, Euro Energies, Saint Symphorien, France and Ignis®, Greenagro, Katowice, Poland). Miscanthus was used as an additional biomass type. The wood pellets were ground for two minutes, using an A 10 basic mill (IKA®-Werke GmbH & CO. KG, Germany) with a water-cooling system at approximately 15°C to prevent thermal alteration.

2.2. Experimental methods

A small amount of ground wood pellets (approx. 0.4±0.1 mg) was introduced in the hollow part of a cylindrical glass capillary with 10 cm length and a diameter inferior to 1 mm. This glass tube was closed by a clean piece of a quartz fiber filter and introduced into the desorption and ionization unit of the mass spectrometer. The presence of the quartz filter in the glass capillary tube induced a delay of evaporation of the sample. Such delay was found beneficial to avoid high ion currents during the thermo-desorption process, thus ensuring regular ion transmission and acquisition [32]. The start of the thermo-desorption and pyrolysis process was prompted by a heated gas stream. Each sample was recorded in triplicate on both mass spectrometric platforms.

FT ICR experiments were performed using a 12T SolariX XR FTMS (Bruker Daltonics). The sample introduction was performed by utilizing the Bruker Daltonics direct inlet probe (DIP), coupled with an atmospheric pressure chemical ionization source (APCI), operated in positive ion mode. Source parameters were chosen to ensure a robust, sensitive, and reproducible analysis of the biomass samples. The nitrogen nebulizer gas was set at a pressure of 3 bar and 400 °C and a nitrogen drying gas flow of 2 L/min at 200 °C. The corona current was set to 3 µA (Table A.1a for source and acquisition parameters). A mass range of *m/z* 122.8 to *m/z* 1,000 was chosen for this study. The analog image current, or transient, was digitized with 2 million data points resulting in the recording of a 0.7 s time-domain signal, which was transformed into the corresponding frequency domain by Fourier transform (after one zero-fill and full-sine apodization). As resolving power scales with transient length, this 0.7 s transient allowed a compromise between the scan frequency of the thermo-desorption profile, which lasts below 4 min, and the resolving power required to differentiate the common isobaric $C_cH_hN_nO_o$ compounds. A resolution of 400,000 was obtained at *m/z* 200. External *m/z* calibration of mass spectra was performed using a polycyclic aromatic hydrocarbon (PAH) standard mixture (Supelco EPA 610, Sigma Aldrich) containing 16 different PAHs and measured with the same instrumental conditions. Internal calibration was performed on an average spectrum generated over the complete analysis using a well-identified series of oxygen-containing compounds (Table A.2).

Ion mobility experiments were performed on a Synapt G2 IMS Q-TOF mass spectrometer (Waters) equipped with an atmospheric solid analysis probe (ASAP), APCI source, and a traveling wave ion mobility (TWIMS) cell. Analyses were performed in positive mode. The source and probe temperature were set to 140°C and 650°C, with a cone gas flow of 20 L/h, and a desolvation gas flow at 1,200 L/h (Table A.1b for source and acquisition parameters). Sampling and extraction cone voltage were set to 20 V and 6 V, respectively, and corona current was set at 30 µA. These ASAP parameters were chosen toensure optimal degradation and ionization of studied biomasses. They

were different from the DIP APCI parameters because of probe and source geometry differences. The IMS parameters were set as following: helium cell flow at 180 mL/min, IMS cell nitrogen flow at 70 mL/min, wave velocity at 350 m/s and wave height at 15 V. Mass spectra were recorded over a range of *m/z* 50-1200. A resolution of 35,000 was obtained at *m/z* 200. External *m/z* calibration was performed using a sodium formate solution. Internal lockmass calibration was performed with an abundant ion from the lignin degradation ($C_{10}H_{12}O_3^{+\bullet}$ ion, *m/z* 180.0786) using MassLynx 4.1 (Waters Corporation). All experiments were recorded in random order to avoid systematic bias from the measurement devices. CCS determination for non-uniform electric field instruments, such as traveling wave ion mobility mass spectrometry (TWIMS), requires a calibration using compounds with known CCS[33]. Here, calibration was performed using two sets of calibrants: polyalanine [34] and a mixture of polycyclic aromatic hydrocarbon (PAH) [35]. Polyalanine was purchased from Sigma-Aldrich (Saint Quentin Fallavier, France). The polyalanine calibrant solution was prepared from a stock solution (1 mg/mL in water/acetonitrile (1/1, v/v)) diluted to 10^{-5} mol/L in water/acetonitrile/acetic acid (49.5/49.5/1, v/v) as described elsewhere [36]. The solution was analyzed using positive electrospray ionization using the parameters shown in Table A.1c. The EPA 525 PAH Mix (Table A.3) was purchased from Sigma-Aldrich (Saint Quentin Fallavier, France). The PAH calibrant solution was prepared from a stock solution (500 mg/L) diluted to 0.3 mg/L in toluene and analyzed using direct infusion in positive APCI and APPI mode (Table A.1d for parameters). Note that because TWIMS is the ion mobility technology used and it is performed in nitrogen drift gas, the calibration used for collision cross section determination is performed using CCS in nitrogen, and the collision cross sections are termed $^{TW}CCS_{N2}$.

Moreover, a set of 12 molecules (Table A.4), putatively identified in the wood pyrolysis process, were analyzed using direct infusion APCI IM-MS from 50 µM solutions in methanol. Nominal mass isolation of specific ions within the quadrupole was performed during analysis of the standard molecules. MS/MS experiments were performed on four of these ions and those obtained from the biomass pellet pyrolysis products. The fragmentation was performed in a collision trap prior ion mobility separation using a collision voltage of 15 V.

2.3. Data processing

For ASAP IMS TOF, raw files were directly processed by self-written MATLAB routines, and molecular assignation was performed using the raw formula $C_{6\text{-}100}H_{6\text{-}200}O_{0\text{-}10}$, double bond equivalent below 25 and H/C ratio between 0.4 and 2.8. Nitrogen was removed from the elemental composition, as the manual examination of the spectra revealed a negligible percentage of molecular attributions included a nitrogen atom. A maximum error of 50 ppm was allowed on the *m/z* values. At least 95% of the total ion intensity was attributed to molecular formulas.

The lists of attributed signals were further treated with MATLAB to create a list of molecular formulas common to at least two out of the three replicates. OriginPro (2016) and MATLAB were used for visualization of the data.

This filtered list of signals and their elemental composition were compared via multivariate data analysis. Principal component analyses (PCA) were performed for the ASAP IM-TOF MS data. All attributions were considered, and attributions not found within a sample were set to zero intensity. An excel file with all the attributions, absolute and normalized intensities is provided as supplementary information. Data were normalized using power transformation (square root) to correct for heteroscedasticity and do pseudo scaling [37]. The resulting scores and coefficient data,

combined with the elemental composition attribution, were used for visualization. In this respect, score data are linked to the experiments (replicates and sample type) and coefficient data to the individual elemental compositions (molecular profile).

Ion mobility peaks were extracted using TWIM extract software from the Ruotolo research group [38]. The extracted data were fitted using symmetric Gauss function with Levenberg Marquardt iteration algorithm using OriginPro 2016 to determine each peak center and full width at half maximum (FWHM). Only mono-modal ion mobility peaks were studied. Moreover, peaks linked with ion statistics below 1000 arbitrary units were discarded since the abundance was too low for the determination of reliable drift time values. The fitted peak centers was used as drift time for the determination collision cross sections in nitrogen $^{TW}CCS_{N2}$.

3. Results and discussion

3.1. Study of ASAP IM-TOF MS profile and mass spectra for beech sample

Figure 1 shows, as an example, one typical mass spectrum averaged between 0 and 4 minutes from the analysis of beech pellets with ASAP IM-TOF MS.

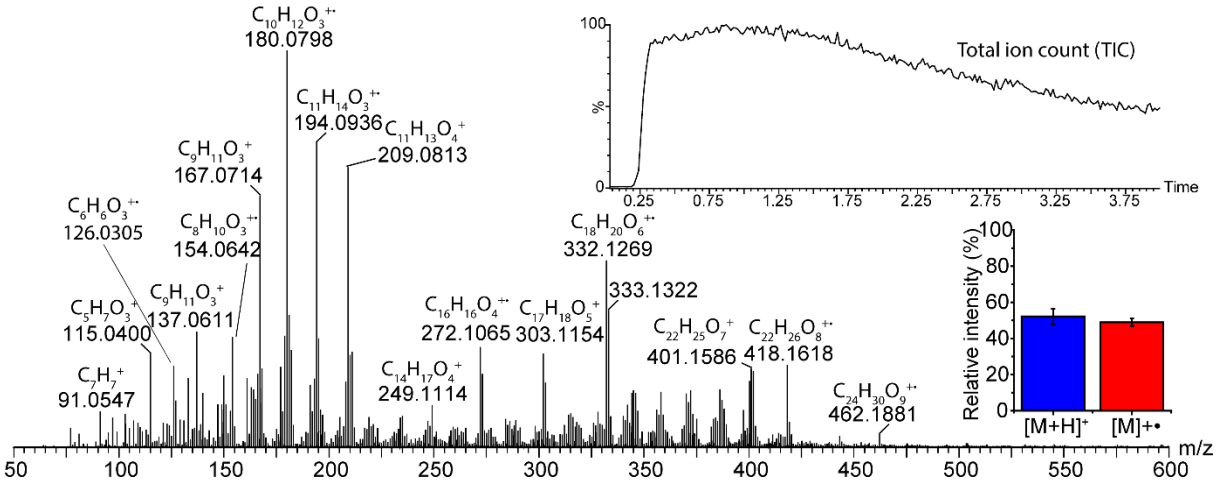

Figure 1: Beech pyrolysis profile and mass spectra from ASAP IM-TOF MS experiment. The pyrolysis profile is displayed as total ion count (TIC) and the insert gives the proportion of protonated ($[M+H]^+$) and radical ($[M]^{+\bullet}$) molecules.

The total ion count profile reached its maximum intensity after 1 min and decayed slowly. Typically, as is shown in the mass spectrum of beech pyrolysis in Figure 1, the mass spectra showed two ion distributions, one distribution in the lower range from *m/z 100-300* and a second distribution in the range of *m/z 300-450*. With beech samples, the most abundant ions in the lower *m/z* range were *m/z 167.0714, 180.0798, 194.0936* and *209.0813*, which were consistent with monomeric lignin degradation products (Table A.5). Also, the *m/z 126.0330* ion could correspond to the radical cation $M^{+\bullet}$ of 5-(hydroxymethyl)-2-furaldehyde, also named hydroxymethylfurfural (HMF), a cellulose degradation product [39]. The 300-450 *m/z* range revealed *m/z 332.1269, 357.1312, 371.1504, 387.1419 and 401.1586 as highly abundant species*. These ions could be attributed to dimeric lignin degradation products, which could be present either as β-β, α-O-4 or β-O-4 linkages [40]. The proportion of protonated (52±4 %) and radical molecules was equivalent. The Table A.5 lists ions detected with their elemental attribution errors and putative neutral structures.

After studying the general ASAP profile and mass spectrometric response, molecular formulas were attributed using the ASAP IM-TOF MS data for the five biomass samples. However, an investigation of isobaric compounds was needed to ensure the reliability of the molecular attribution obtained with the mass resolution of the TOF analyzer. FTICR, with its ultra-high resolution and high mass accuracy, was used for that purpose. A direct insertion ionization source equivalent to ASAP, the DIP APCI source, was used to obtain comparable analytical conditions. . Two ion distributions were observed for both ASAP IM-TOF MS and DIP FTICR (Figure A.1). The distribution in the lower range from *m/z* 100-300 was more intense with ASAP and the second distribution in the range of *m/z* 300-450 was more intense with DIP. Moreover, a higher number of different ions were found with DIP FTICR compared to ASAP IM-TOF MS. These variations are expected to result from both geometry differences between the two probes and differences between the mass analyzer. The TOF mass analyzer is faster compared to FTICR MS but less sensitive when operated in high resolution mode and reaches a lower resolution and dynamic range. The ASAP probe is heated to a set temperature (650°C) while in DIP only the nebulizer and drying gas are heated. Moreover, we cannot monitor the exact temperature and do not control how the heat transfers in either devices. . The proportion of protonated molecules was higher for DIP APCI compared to ASAP. A modification of the ASAP ionization process was then needed to have a proportion of protonated molecules similar to DIP APCI, making the mass spectra more comparable. For that purpose, a vial of pure methanol was directly placed in the ASAP source (Figure A.2).

Figure 2 shows the overlay of DIP APCI FTICR and ASAP IM-TOF MS mass spectra for four selected nominal masses corresponding to the standard molecules further used in the ion mobility part of this study (Table A.5).

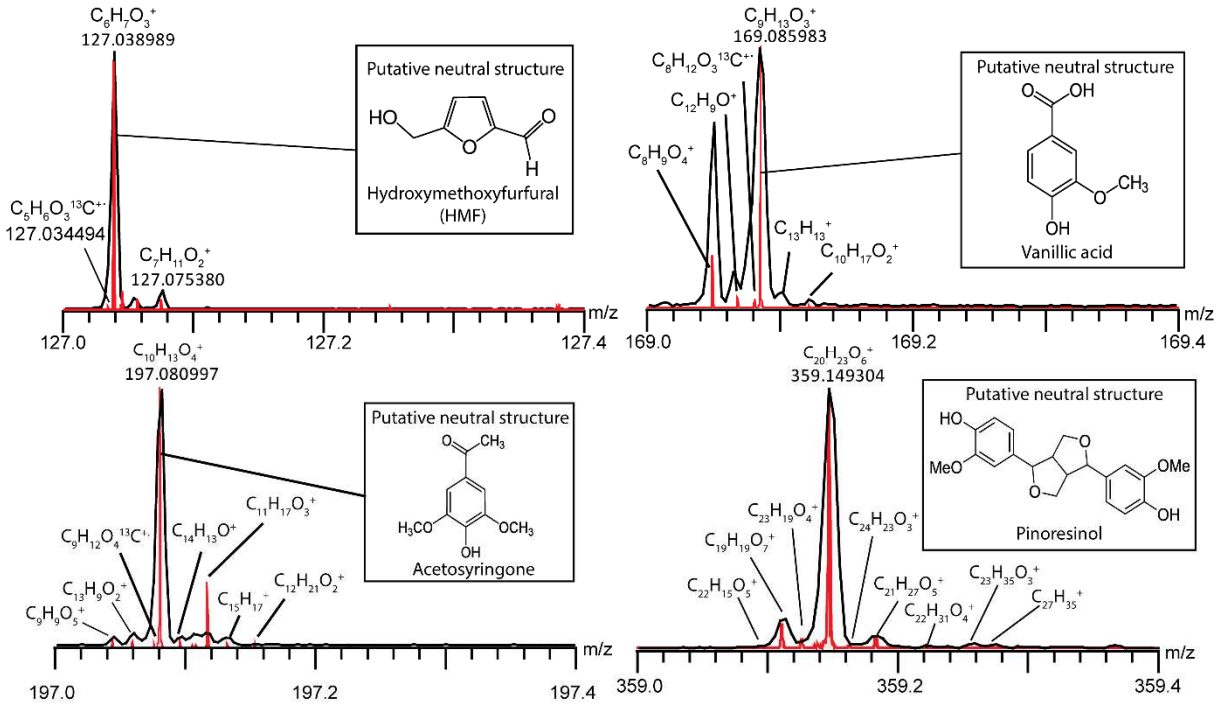

Figure 2: DIP FTICR (red) and ASAP IM-TOF MS (black) mass spectra overlaid at selected nominal masses. Putative neutral structures for selected compounds are shown.

The peaks of the DIP FTICR mass spectra are annotated with the attributed molecular formulas. As apparent in Figure 2, the number of peaks per nominal mass increased with rising *m/z*. The most

intense peak at *m/z 127* was the *m/z 127.03900* peak that could be attributed to $C_6H_7O_3^+$, which could correspond to protonated HMF. An ion at *m/z 127.07537,* attributed to $C_7H_{11}O_2^+$ was also observed in both analytical methods. The only possible isobaric interference could arise from another signal at *m/z* 127.03449; which was attributed to the ^{13}C isotope from a $C_6H_6O_3^{+\bullet}$ radical cation. Similar observations were obtained throughout the mass spectra as shown for odd *m/z* nominal value ions *m/z* 169 and *m/z 197*, where low-intensity ^{13}C isotopes of radical cations were only resolved in DIP FTICR data. However, when $[M+H]^+$ ions are more intense compared to $M^{+\bullet}$ ions, isotopic interferences could be observed for even *m/z* nominal value ions (*m/z* 180, 210, 298, 352 in Figure A.3) where ^{13}C isotopes of $[M+H]^+$ may overlap with monoisotopic $M^{+\cdot}$ ions. When ASAP experiments were carried out without using a methanol vial in the source unit, protonated ions were less abundant and thus ^{13}C isotopes of $[M + H]^+$ were less intense in even *m/z* nominal value ions. Only low-intensity ^{13}C isotopes from abundant radical cations could be present as unresolved signals together with less abundant protonated ions in odd *m/z* nominal value ions. Even then, the low abundance of ^{13}C isotopes were not found to cause any significant isobaric interferences so that ASAP IM-TOF MS experiments could be used as well for the determination of molecular markers of hardwood and softwood samples. The negligible influence of isobaric interferences in ASAP IM-TOF MS increased our confidence in the molecular attribution of ASAP IM-TOF MS data even with higher mass errors (around 5 ppm compared to 0.5 ppm with FTICR) and we found the use of methanol in the ASAP source was not needed. In fact, 70% of molecular formulas attributed were found in both conditions (with and without methanol) (Venn diagram in Figure A.4). However, still around 360 specific molecular formulas were obtained when methanol was added or not. We chose not to use methanol so as not to modify of the pyrolysis and ionization processes and decrease isobaric interference for even *m/z* nominal value ions. The finding that the presence of isobaric interferences was negligible, also in odd *m/z* nominal value ions also served as an indication that, when ion mobility was used, the extracted ion mobility spectra of a given *m/z* value should arise from one unique molecular formula rather than a collection of isobaric ions. Only molecular formulas derived from ASAP IM-TOF MS data without methanol were used in the following to compare the biomass samples.

3.2. Molecular mapping of the biomass samples

All ASAP IM-TOF MS data were processed using MATLAB scripts, and a list of molecular attributions for the replicates of each sample was obtained. The Figure A.5 in the supplementary material shows the Venn diagram for all samples and replicates. Around 1,000 molecular formulas were determined for each biomass sample. Moreover, at least 75% of the molecular formulas for the five samples were common to at least three replicates, pointing out the reproducibility of the ASAP method. The ASAP IM-TOF MS molecular formulas were used in graphical representation for the comparison of the biomass samples. The van Krevelen diagram is a graphical representation that provides information on molecular families present in the studied samples by plotting the O/C and H/C molecular ratios of attributed molecular formulas [41]. Figure 3 shows van Krevelen diagram from the molecular formulas of the five biomass pellets analyzed (beech, hickory, Crepito®, Ignis® and miscanthus).

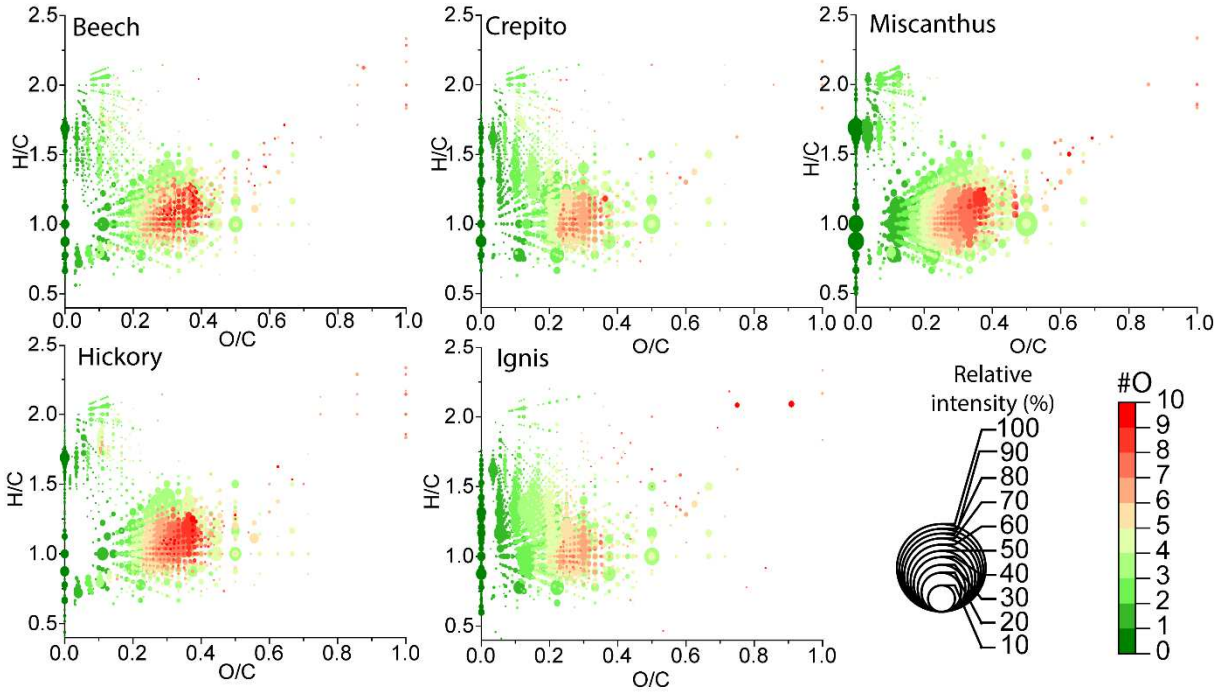

Figure 3: Van Krevelen diagrams from the analysis of five lignocellulosic biomass samples. The number of oxygen atoms is color-coded and the relative intensity is represented by the size of dots. The presented data is based on the average of three replicates.

The beech and hickory hardwood samples showed similar molecular families. One molecular family was found with H/C ratio between 1.3 and 2.3, O/C ratio between 0 and 0.2 and a low number of oxygen atoms (between one and three). Such ratios and characteristics point towards saturated compounds such as fatty acids and fatty ester. A second molecular family was observed with H/C ratio between 0.75 and 1.5, O/C between 0.1 and 0.5 and a number of oxygen atoms from one to ten. This molecular family corresponded to lignin degradation products with lignin monomeric compounds at low O/C ratio and lignin dimeric compounds at higher O/C ratio. Lignin degradation products are expected to contain either p-coumaryl (H unit), coniferyl (G unit) or sinapyl (S unit) building blocks.

Crepito® and Ignis® softwood samples exhibited different molecular characteristics. One molecular family was found with lower H/C ratio between 0.75 and 1.5 and low O/C ratio between 0.05 and 0.2 and a number of oxygen atoms between one and four. Such characteristics are in line with wood extractable compounds, such as terpenoid, flavonoid and resins [42]. Such extractable compounds were not found in the beech and hickory hardwood samples, showing differences between the biomass species. Similarly to hardwood, a second molecular family, corresponding to lignin degradation products, was found in softwood samples with H/C ratio between 0.75 and 1.5, O/C between 0.1 and 0.4 and a number of oxygen atoms between one and eight. Small differences were observed between hardwood and softwood for that molecular attribution family. In fact, more compounds were found in hardwood samples than in softwood, and these compounds contained a higher number of oxygen atoms. Also, the relative intensity of the lignin degradation products was higher for hardwood samples [43].

The miscanthus sample was similar to the hardwood samples. The use of the van Krevelen diagram allowed differentiation of the five biomass samples based on a fingerprinting approach. However,

further data processing, by means of principal component analysis (PCA), is required for data reduction and to extract molecular markers specific to the different wood species.

3.3 Multivariate statistical analysis for the differentiation of biomass samples

Molecular attributions and the normalized intensities from every sample were merged into one Table. This table was submitted to principal component analysis (PCA) and the score plot is shown in Figure 4.

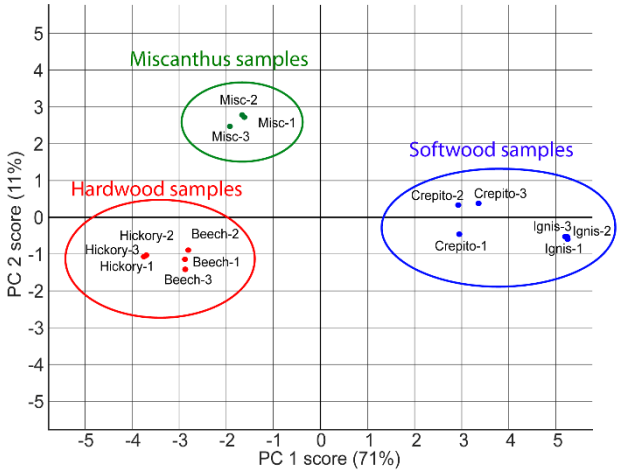

Figure 4: PCA Score plot visualizing the first two principal components obtained from ASAP IM-TOF MSPCA (around 82% of the total variance). Soft wood samples are given in blue, hardwood samples given in red and miscanthus sample displayed in green.

The first component of the PCA accounted for 71% of the total variability of the samples. The second component only accounted for 11% of the total variance. A clear separation could be observed between the softwood samples, with positive PC1 score, hardwood and miscanthus, with negative PC1 scores. The first component showed similarities between hardwood and miscanthus. The separation of samples within the first component was used to explore the chemical differences between the samples. These differences are expected to derive from the relative ion abundance of marker species of a certain biomass type. The PC1 coefficients (also called loading data) were combined to the corresponding molecular attribution using van Krevelen diagram to better visualize the chemical differences between biomass samples. Figure 5 shows a van Krevelen diagram obtained from PCA data, with PC1 coefficients as color code and dot size as normalized summed intensity. Positive PC1 coefficients, represented in red, corresponded to molecular formulas more abundant in softwood. Negative PC1 coefficients, represented in green, corresponded to attributions more abundant in hardwood and miscanthus. The molecular attributions represented in yellow had similar intensities between hardwood, softwood and miscanthus.

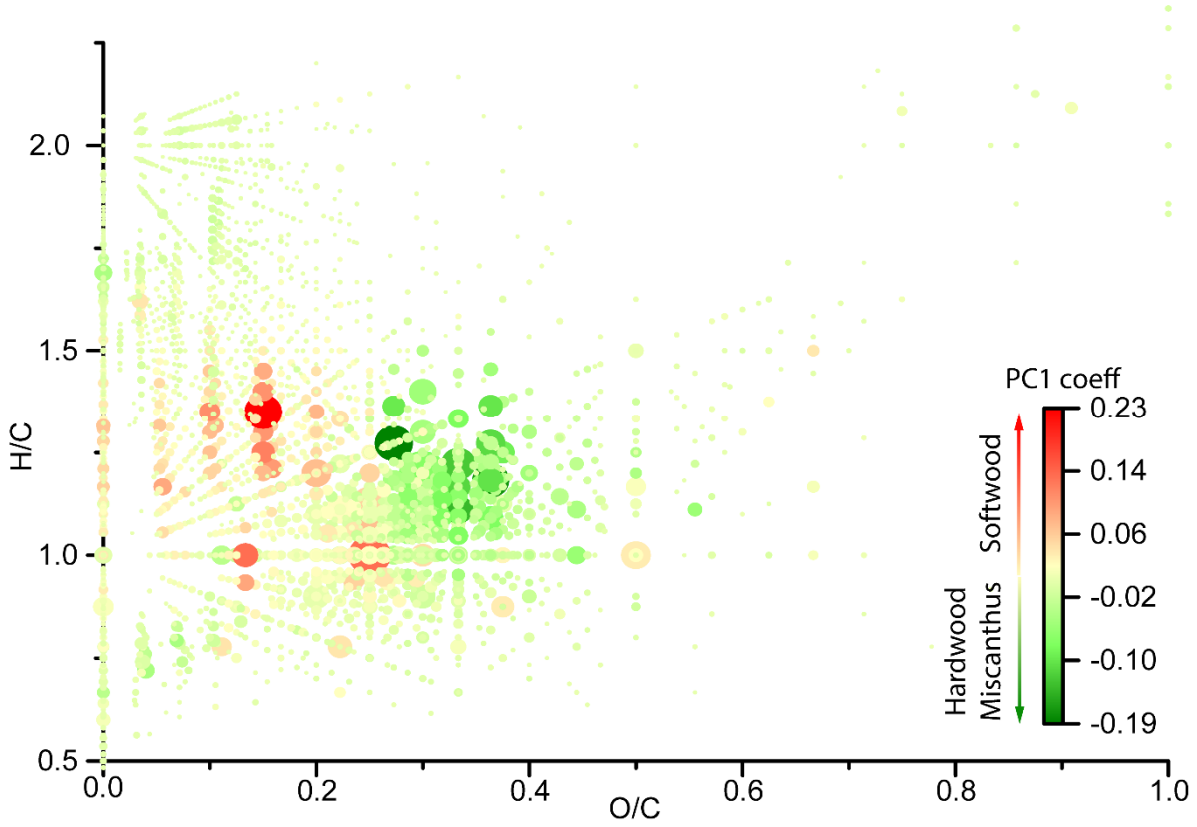

Figure 5: Modified van-Krevelen plot obtained from ASAP IM-TOF MS PCA data. The size of dot corresponded to the ion normalized summed intensity and the colormap corresponded to the PC1 coefficients.

Fatty acids and esters (appearing at H/C ratios above 1.5 and low O/C ratios) exhibited PC 1 loadings close to zero, showing that these compounds were found in the same proportion in the five biomass types or have high standard deviation from the replicates, making them not significant in the PCA. Wood extractable compounds that have molecular formulas with H/C ratio between 1.0 and 1.6 and low O/C ratio (below 0.2) appeared with highly positive PC1 coefficients, confirming a higher abundance of these compounds in softwood samples. Among lignin degradation products, molecular formulas with lower H/C ratio (0.8<H/C<1.0) and slightly higher O/C ratios that correspond to p-hydroxyphenyl units (H) appeared with positive PC1 coefficients. Whereas lignin degradation products with molecular formulas of higher H/C and O/C ratios (0.9<H/C<1.5 and 0.25<O/C<0.4) presented mostly negative PC1 coefficients. These ratios correspond to lignin degradation products containing syringyl units (S). The presence of S unit lignin degradation products was consistent with the higher proportion of synapyl alcohol monomer in hardwood species compared to softwood, already reported [44]. The molecular formulas with the ten highest and the ten lowest PC1 coefficients are listed in Table A.6a and A.6b with putative neutral structure and their family. Compounds of the terpenoid family had positive PC1 coefficients and were therefore thought to characterize softwood. Molecules related to the S unit lignin monomer that had negative PC1 coefficients were found to characterize hardwood and miscanthus. However, at this level of data analysis, only molecular formulas were obtained, and we sought to describe discriminative ions further using ion mobility based on drift time and determination of their collision cross section (CCS_{N2}).

3.4 Collision cross section of hardwood and softwood pyrolysis molecular markers

The CCS determination was performed on sixty ions from biomass thermo-desorption and pyrolysis products. This number of ions was intended to initiate the creation of an experimental CCS database for wood degradation markers. Half of these ions were found to be characteristic to softwood samples (highest PC1 coefficients). These thirty attributions with the highest PC1 coefficient corresponded to biomass extractables. Most of these extractables were specifically found in softwood. The second half of the sixty chosen ions were found to be characteristic to hardwood samples (lowest PC1 coefficients). These thirty ions corresponded to monomeric and dimeric lignin degradation products. Some of these markers were below the detection limit or at very low abundance for the softwood samples.

The drift times values from the sixty biomass markers were determined from ion mobility peaks after a Gaussian fit. A calibration was performed to convert drift times to $^{TW}CCS_{N2}$ using compounds of known collision cross section. It is recommended to choose calibrants with similar *m/z* and CCS range as well as similar structures to the studied ions [45]. A mix of polycyclic aromatic hydrocarbons (PAH) was chosen as calibrant [35] since their structures are close to wood degradation products. Figure 6a shows the PAH CCS calibration curve (R^2 0.9966). The resulting $^{TW}CCS_{N2}$ values of the biomass pyrolysis markers are listed in Table A.7a and $^{TW}CCS_{N2}$ *vs. m/z* plot is shown in Figure 6c. Half of the $^{TW}CCS_{N2}$ values from the biomass pyrolysis markers were very similar the CCS of the PAH, confirming their shape similarity. However, the PAH mix only covered a range of *m/z* 50-278, so that the CCS of markers with higher masses needed to be extrapolated. To overcome this *m/z* and CCS range discrepancy, another set of CCS calibrant was used to extend the mass and CCS range. Polyalanine was used for that purpose since this CCS calibrant is well established [34]. However, calibration has been shown to differ with the choice of calibrants [36]. Figure 6b shows the polyalanine CCS calibration curve (R^2 0.9999). The slope was different from the calibration line obtained with the PAH mix. The $^{TW}CCS_{N2}$ values, derived from this calibration for the biomass pyrolysis markers, are listed in Table A.7b and $^{TW}CCS_{N2}$ *vs. m/z* plot is shown in Figure 6d. The polyalanine covered a *m/z* range from 232 to 587. However, polyalanine is structurally very different from biomass pyrolysis markers as attested by their very different CCS_{N2} values depending on *m/z*. Nevertheless, we chose to retain both calibrations but wish to point out that our $^{TW}CCS_{N2}$ determinations are relative to one chosen calibrant: PAH for low mass compounds and polyalanine for higher mass compounds.

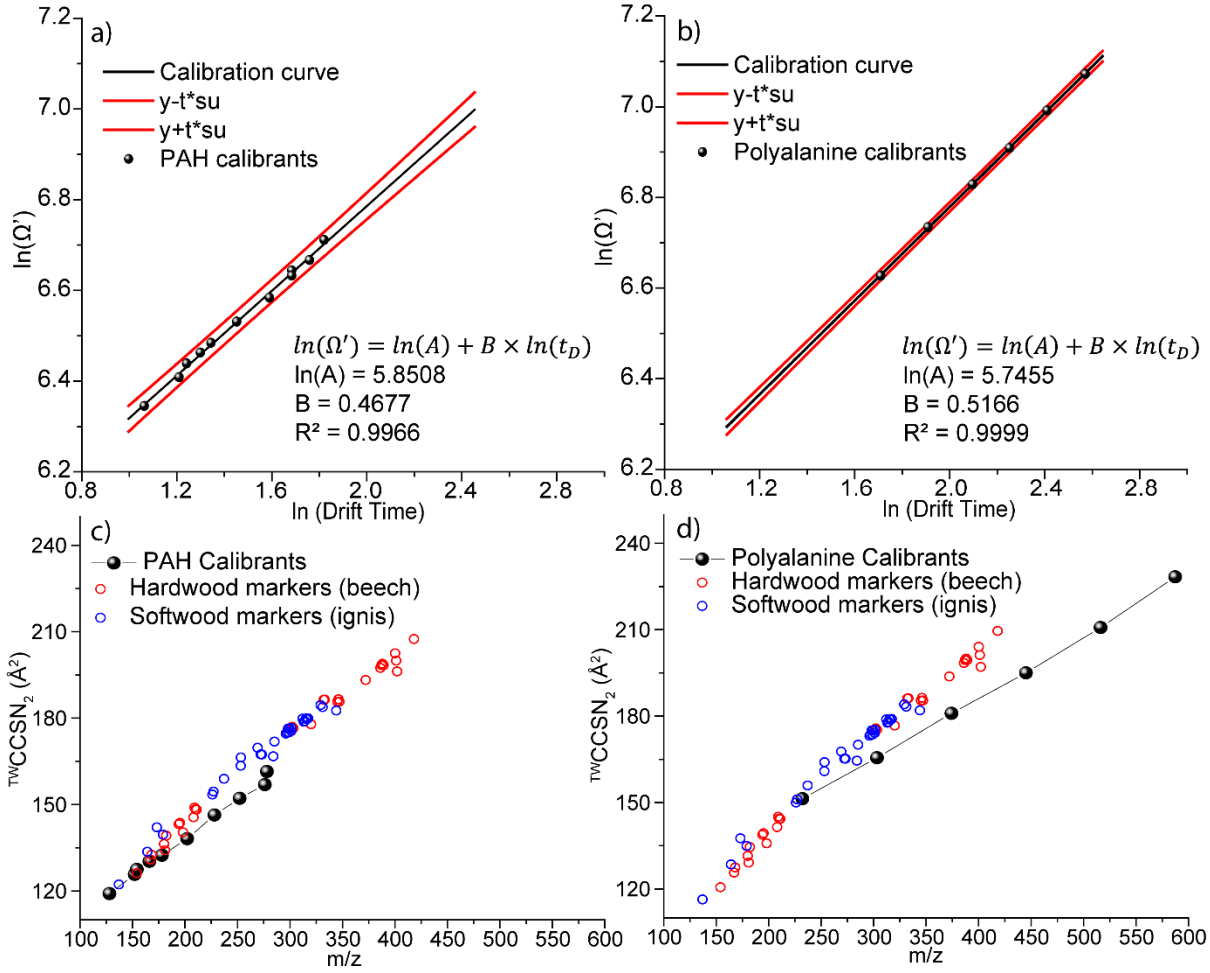

Figure 6: CCS calibration curve and $^{TW}CCSN_2$ vs. *m/z* plots for the description of softwood and hardwood plus miscanthus molecular markers. a) and c) corresponded to CCS PAH calibration and $^{TW}CCSN_2$ vs. *m/z* plot including PAHs calibrants. b) and d) corresponded to CCS polyalanine calibration and $^{TW}CCSN_2$ vs. *m/z* plot including polyalanine calibrants.

The mean RSD values of the $^{TW}CCS_{N2}$ from the three replicated experiments were below 0.5% for all five biomass samples. $^{TW}CCSN_2$ differed between polyalanine and PAH mix CCS calibration. These differences were higher at low *m/z* ratio (up to 6 Å²). The $^{TW}CCS_{N2}$ values determined for each ion were similar for all the wood species, with maximum differences of 2 to 3 Å². These similarities in CCS showed that the five biomass samples most likely contained similar isomeric species. Further analysis was done to study the isomeric diversity of wood pyrolysis compounds using standard molecules.

3.5 Determination of collision cross sections of standard molecules and comparison with wood degradation products.

To have a better structural insight on wood degradation products, twelve standard molecules, which are markers from wood degradation [46], were analyzed using ion mobility mass spectrometry (Table A.3). These standards were chosen according to the molecular families found for wood degradation products [47]. Two degradation products of cellulose were studied, furfural (FF) and hydroxymethylfurfural (HMF), which result from incomplete degradation of cellulose. Abietic acid is an extractable found in coniferous wood. The other standard molecules studied are monomeric wood degradation products reported in the literature [46] monomers of the G, S and H

units, which are lignin markers. The extracted ion mobility spectra of the ions obtained with these standard molecules were compared to the ions obtained from the biomass samples (Figure 7). Table 1 shows the $^{TW}CCS_{N2}$ values from the standard molecules and the corresponding $^{TW}CCSN_2$ from wood pyrolysis using PAH mix for CCS calibration. The mean RSD of three analytical replicates was below 0.3% for all the wood species and the standards.

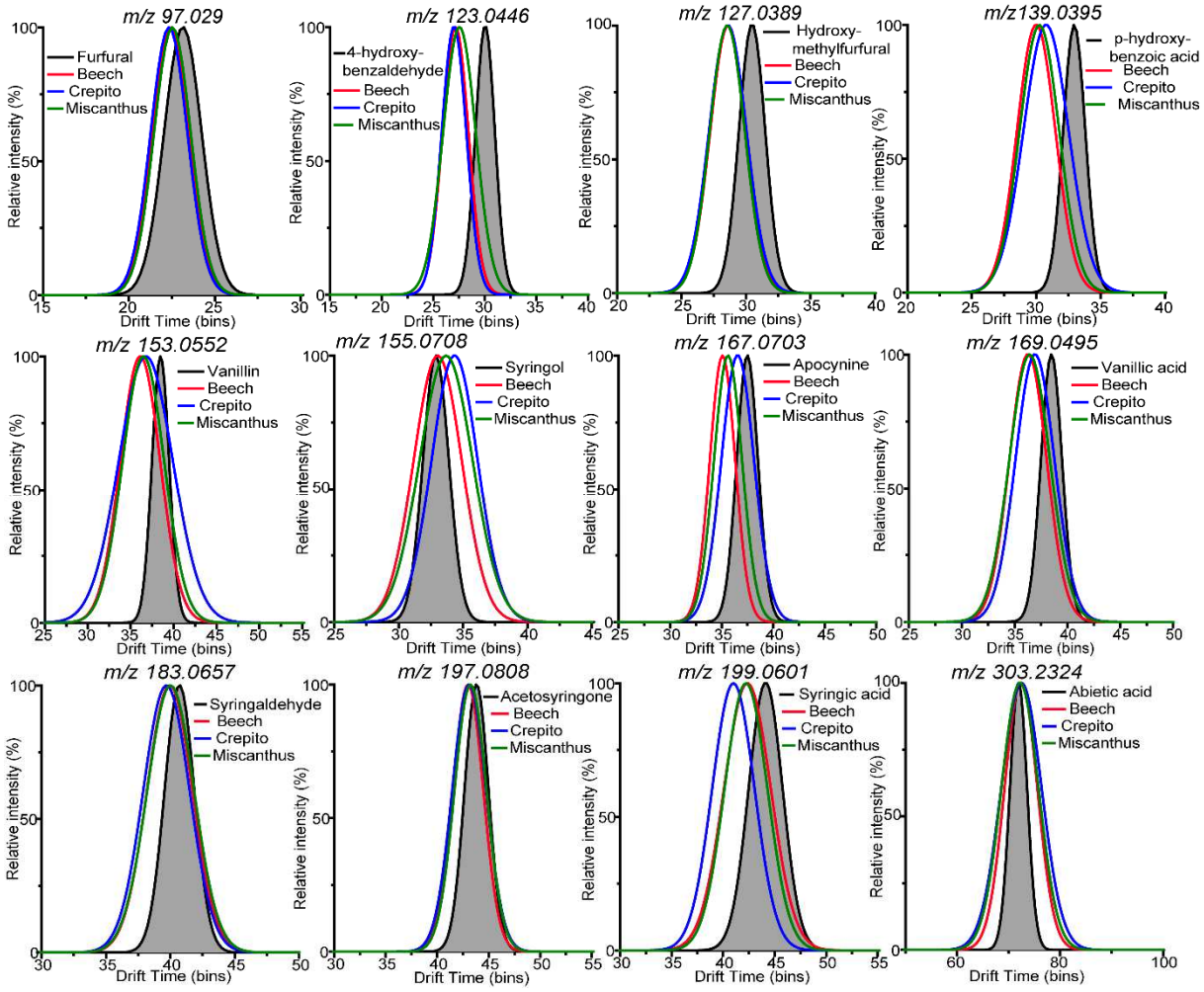

Figure 7: Gaussian fitted extracted ion mobility peaks from wood pyrolysis products. Ordinate was the relative intensity and the abscissa is the drift time measure in bins. The black line with grayed area represents the standard molecule, the red line displays beech sample (hardwood), the blue line displays Crepito® sample (softwood) and the green line, visualize miscanthus sample.

Drift time distribution was found to be within the experimental distribution of the biomass material for all investigated standards. Nonetheless, the standards only account for a fraction of the isomeric diversity and the biomass materials exhibit significantly broader distributions.

Significant deviations between standard and biomass sample in drift times were observed for *m/z 123.0446*, *127.0389* and *139.0395,* which corresponded to protonated 4-hydroxybenzaldehyde, hydroxymethylfurfural (HMF), p-hydroxybenzoic acid.

In most cases, the ions from the chosen standard molecule had larger drift times than the ions from the wood samples, which led to $^{TW}CCS_{N2}$ values 2 to 4 Å^2 higher for the ions from the chosen standard

compared to the ions from the pellet samples. Such differences could arise from a different position of the substituents in these low molecular weight compounds. For all other ions, drift time values were more similar between the standard molecules and the wood degradation products. However, the full width at half maximum (FWHM) was generally higher for the wood degradation products than the chosen standard molecules. The largest increase in FWHM in the biomass materials were found for *m/z 139.0395*, *155.0708*, *169.0495* and *303.2324,* which corresponded to p-hydroxybenzoic acid, syringol, vanillic acid and abietic acid. A higher FWHM could indicate the presence of several unresolved isomers in the wood samples, compared to the chosen standard. In literature, the FWHM is used as a measure for isomeric diversity and thus expose valuable structural information [48].

To further characterize the molecular structure of the wood pyrolysis products and probe the presence of isomers, MS/MS experiments were performed on four of the selected standard molecules.

Table 1: $^{TW}CCSN_2$ values from the TWIMS analysis of twelve molecular standards and comparison with wood pyrolysis products. The twelve standard molecules were chosen according to the molecular families found for wood degradation products. The CCS values were determined in triplicate using PAH mix as CCS calibrant, for standard and the biomass samples and the RSD values are displayed.

Standard name	Origin	Formula	$[M+H]^+$ *m/z*	Standard molecules $^{TW}CCS_{N2}$ (Å²) Mean value	Standard molecules $^{TW}CCSN_2$ RSD (%)	Beech $^{TW}CCSN_2$ (Å²) Mean value	Beech $^{TW}CCSN_2$ RSD (%)	Hickory $^{TW}CCSN_2$ (Å²) Mean value	Hickory $^{TW}CCSN_2$ RSD (%)	Crepito® $^{TW}CCSN_2$ (Å²) Mean value	Crepito® $^{TW}CCSN_2$ RSD (%)	Ignis® $^{TW}CCSN_2$ (Å²) Mean value	Ignis® $^{TW}CCSN_2$ RSD (%)	Miscanthus $^{TW}CCSN_2$ (Å²) Mean value	Miscanthus $^{TW}CCSN_2$ RSD(%)
Furfural	Cellulose degradation	C5H4O2	97.029	110.03	0.09%	110.53	0.09%	110.49	0.04%	110.54	0.29%	110.36	0.02%	110.79	0.08%
Hydroquinone	Lignin monomer degradation H unit	C6H6O2	111.0446	111.01	0.19%	116.40	0.07%	116.44	0.05%	116.10	0.09%	116.09	0.06%	116.37	0.17%
4-Hydroxybenzaldéhyde	Lignin monomer degradation H unit	C7H6O2	123.0446	122.27	0.07%	118.10	0.11%	118.04	0.04%	117.88	0.15%	117.85	0.05%	119.15	0.10%
Hydroxymethylfurfural	Cellulose degradation	C6H6O3	127.0389	122.71	0.01%	120.52	0.25%	120.51	0.13%	121.07	0.35%	120.79	0.02%	120.95	0.17%
p-hydroxybenzoic acid	Lignin monomer degradation H core	C7H6O3	139.0395	126.49	0.01%	122.41	0.15%	122.37	0.16%	124.79	0.71%	123.44	0.07%	123.21	0.09%
Vanillin	Lignin monomer degradation G core	C8H8O3	153.0552	129.44	0.05%	127.19	0.31%	126.98	0.20%	129.75	0.07%	129.66	0.03%	129.02	0.04%
Syringol	Lignin monomer degradation S core	C8H10O3	155.0708	125.41	0.10%	126.88	0.26%	126.59	0.16%	129.35	0.23%	129.55	0.06%	128.36	0.05%
Apocynine	Lignin monomer degradation G core	C9H10O3	167.0703	132.86	0.02%	130.17	0.06%	130.05	0.03%	132.29	0.39%	133.27	0.12%	131.00	0.14%
Vanillic acid	Lignin monomer degradation G core	C8H8O4	169.0495	134.38	0.08%	132.15	0.45%	131.92	0.28%	133.05	0.54%	132.75	0.33%	133.25	0.49%
Syringaldehyde	Lignin monomer degradation S core	C9H10O4	183.0657	137.45	0.07%	137.50	0.11%	137.43	0.07%	137.16	0.10%	136.78	0.06%	137.69	0.06%
Acetosyringone	Lignin monomer degradation S core	C10H12O4	197.0808	141.92	0.24%	141.79	0.08%	141.76	0.06%	142.04	0.04%	141.55	0.10%	142.11	0.05%
Syringic acid	Lignin monomer degradation S core	C9H10O5	199.0601	141.98	0.22%	140.47	0.16%	140.69	0.11%	139.03	0.42%	138.30	0.14%	140.38	0.09%
Abietic acid	Wood extractable	C20H30O2	303.2324	176.34	0.12%	177.51	0.15%	177.31*	0.06%*	177.19	0.35%	177.04	0.48%	177.63*	0.27%*

* Fitted peak height<1,000 arbitrary units

3.6 MS/MS experiment on standard molecules and wood degradation products

The four molecules chosen for MS/MS experiment were 4-hydroxybenzaldehyde (*m/z 123.0446*), hydroxymethylfurfural (*m/z 127.0389*), apocynin (*m/z 167.0703*) and acetosyringone (*m/z 197.0808*). These compounds were chosen for this experiment since they are representative of lignin and cellulose degradation products. 4-hydoxybenzaldehyde is a lignin H-unit compound, apocynin is a lignin G-unit compound, acetosyringone is a lignin S-unit compound and hydroxymethylfurfural (HMF) is a cellulose degradation compound.

Figure 8 shows the comparison between MS/MS experiments of the HMF standard and MS/MS experiment of *m/z 127.0389* from the ASAP analysis of beech at two different collision voltages applied in the trap cell placed before ion mobility separation.

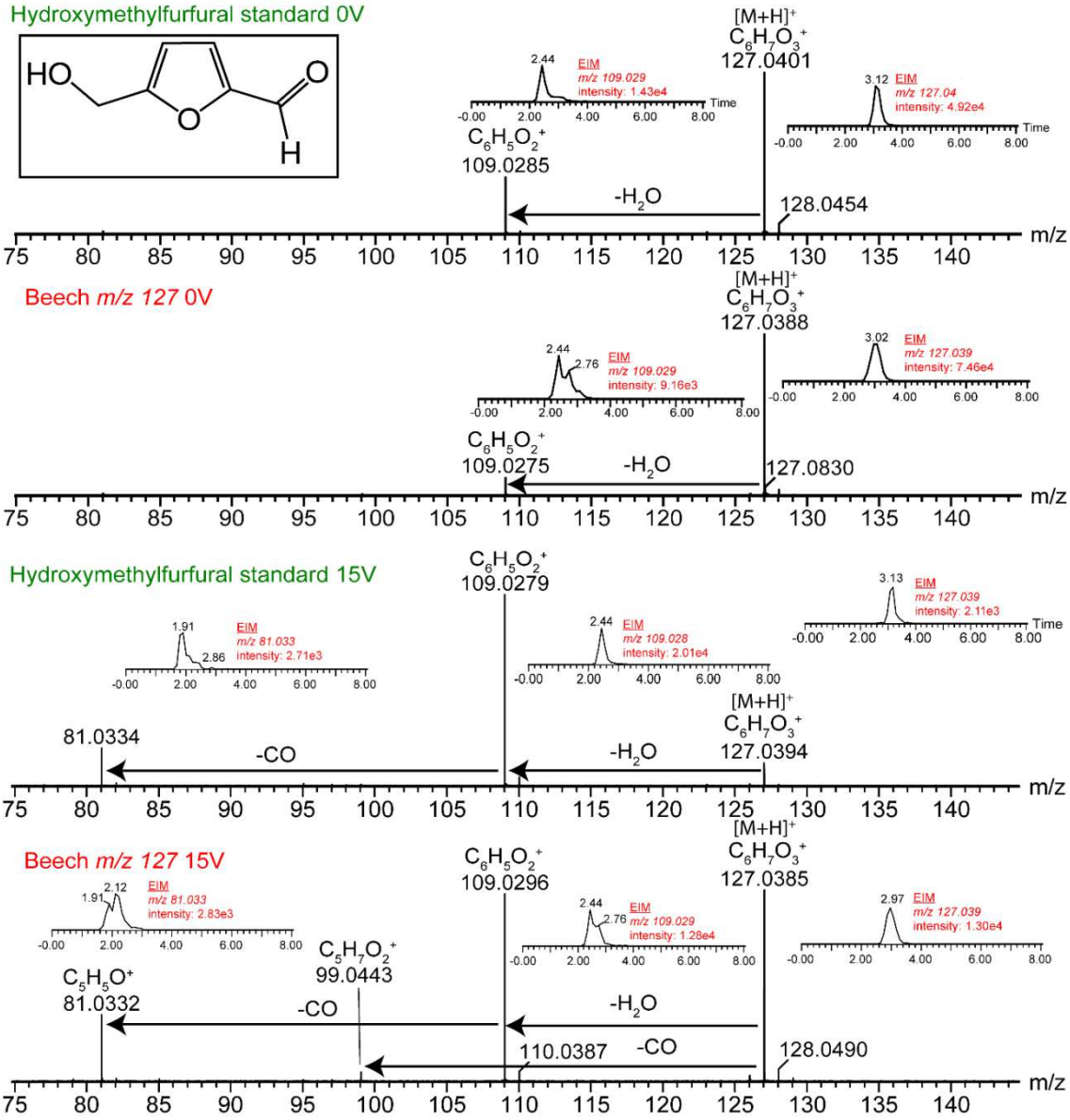

Figure 8: MS/MS spectra from the analysis of molecular standard and wood pyrolysis products. Two collision voltages were used: 0 V and 15 V. The upper spectrum for each collision voltage was from standard molecule and the lower spectrum, from the beech pellet pyrolysis. The extracted ion mobility was added for the most abundant peaks.

Fragmentation was observed even at 0 V collision voltage, due to a small voltage difference (4 V) required for ion transmission. The fragmentation pattern at 0 V was similar between HMF standard and beech pellet degradation: a dominant water loss signal was observed, followed by a subsequent loss of carbon monoxide. These losses correspond to cleavages of the furan substituents of HMF. The same fragments but more intense were observed for the HMF standard with 15 V collision voltage. Moreover, an *m/z* 99.0511 ion emerged in the beech pellet ASAP analysis at 15 V collision voltage. This ion is expected to result from a carbonyl loss from the *m/z 127.0401* ion ($C_6H_7O_3^+$).

The presence of an additional fragment ion, though small, could arise from the presence of isomeric diversity for the $C_6H_7O_3^+$ ion in the beech pyrolysis products. This hypothesis was strengthened by the observation of several differences in the ion mobility profiles of the fragment ions. The *m/z 109* extracted ion mobility with 15 V trap collision voltage showed two peaks for beech pyrolysis at 2.44 ms and 2.76 ms, while the *m/z* 109 ion from HMF showed only one peak at 2.44 ms. Still, the 2.44 ms peak was present in both samples, confirming the presence of HMF in beech pyrolysis products. The *m/z 81* ion extracted ion mobility was also different between beech and HMF standard. For a collision voltage of 15 V, two peaks were observed at 1.91 ms and 2.33 ms for beech, whereas HMF standard had one peak at 1.80 ms with a small tailing at 2.44 ms. We hypothesize maltol as one of the possible isomers found in wood pyrolysis products, in addition to HMF.

The MS/MS spectra for 4-hydroxybenzaldehyde (*m/z 123.0446,* $C_7H_7O_2^+$), apocynin (*m/z 167.0703,* $C_9H_{11}O_3^+$) and acetosyringone (*m/z 197.0808,* $C_{10}H_{13}O_4^+$) are shown in Figure A.6a, A.6b and A.6c, respectively. The fragmentation pattern of 4-hydroxybenzaldehyde (Figure A.6a) showed a loss of a carbonyl function leading to *m/z 95,* which was also observed in the *m/z* 123 ion from the beech pellet. An additional fragment at *m/z 77* was observed for the beech pellet ion. The *m/z 123* extracted ion mobility peak was larger for beech with slight tailing observed.

The fragmentation pattern for apocynine standard and beech pellet ion at m/z *167* (Figure A.6b) at a collision voltage of 15 V, showed two fragments ions *m/z 125* and at *m/z 110,* corresponding to the loss of a ketene molecule followed by the loss of a methyl radical. Different fragment ions (*m/z* 107, 123, 135 and 149) were observed for the beech sample. These additional fragment ions could be due to another precursor ion since the resolution of the quadrupole selection is limited as shown by the presence of an ion at *m/z 166* corresponding to the radical ion from $C_9H_{10}O_3$ in the MS/MS spectrum at 0 V collision voltage of the beech pellet ion at m/z *167*. However, differences in drift time of the *m/z* 167 ion, although difficult to interpret, also pointed out that the *m/z* 167 ion from the beech pellet was probably not, or not only apocynine.

For acetosyringone and the associated *m/z* 197 for beech pellet (Figure A.6c) differences were also observed. At a collision voltage of 0 V, *m/z 196* ion was observed only for the beech sample. A higher number of fragment ions for the beech sample was observed when increasing the collision voltage to 15 V. However, similar fragments were observed between the acetosyringone standard and the *m/z* 197 from the beech pellet. These fragments were *m/z 155*, *140* and *109* (loss of a ketene molecule followed by the loss of a methyl radical an a methoxy radical). The extracted ion mobility spectrum from the *m/z 155* fragment ion was different between the two samples: two ion mobility peaks were observed for beech and one peak was observed acetosyringone. This difference showed the presence of isomers within the *m/z 155* fragment ion probably arising from the presence of isomers in the *m/z* 197 precursor ion for the beech pellet.

Consequently, although further investigation would be needed for full characterization, detailed tandem mass spectrometric experiments and ion mobility showed the ions derived from the beech pellet samples demonstrated that in addition to the standard molecules, various other isomeric structures are present in the wood pyrolysis products. As a consequence, for each molecular formula, several isomers should be considered and can be explored by the presented approach

Conclusion

In this study, we present the direct analysis of solids by high resolution mass spectrometry and ion mobility spectrometry for the chemical description of degradation products from various biomass materials. Previously, DIP FTICR MS, giving information on molecular formula, was developed for the characterization of lignocellulosic biomass [32]. However, FTICR MS provided only limited structural information. The addition of ion mobility allowed for the observation of isomeric diversity during the biomass pyrolysis process for a wide variety of biomass types and pyrolysis products.

The analysis involved the use of an ASAP source that, beneficially, yielded *in situ* pyrolysis of the samples. Although the IMS data was obtained from a high resolution time of flight instrument, the absence of isobaric interference was validated and confirmed by FTICR MS.

We could show that the ASAP IMS TOF platform is a powerful tool for the description of the pyrolysis product of biomass samples, giving both molecular formulas and isomeric information within minutes. Comprehensive processing of the ASAP IMS TOF data and multivariate data analysis by PCA allowed for the extraction of molecular markers specific to biomass families involving softwoods, hardwoods and miscanthus. The experimental $^{TW}CCS_{N2}$ of these markers were obtained using ion mobility mass spectrometry. Low $^{TW}CCS_{N2}$ differences were observed between the biomass samples, showing the isomeric similarities. By using standard molecules, it was demonstrated based on tandem mass spectrometry and ion mobility profiles that various isomers are present in the real biomass. In particular, differences in drift time and increase of peak width (FWHM) in the biomass sample could be observed.

The authors believe that ASAP IMS TOF could be a supplemental technique to Py-GC-MS and GC×GC MS adding the drift time dimension, faster analysis time and CCS information. Py-GC-EI-QMS remains the state-of-the-art instrumental platform for the chemical description of the pyrolysis products from lingnocellulosic biomass. Isomeric separation power, (i.e. peak capacity, number of theoretical plates orthogonality, etc), of established gas chromatographic solutions is superior to current ion mobility devices. Comprehensive gas chromatography (GC x GC) offers even higher peak capacity and better separation. Nevertheless, the measurement time of ASAP IM TOFMS is lower allowing for a higher throughput (even though pyrolysis gas chromatography can be automatized with an auto sampler). Thus, one key benefit of the presented approach is its ease of use (no time-demanding optimization of the chromatographic separation conditions for an optimized method) and the rapid measurements. However, the ion mobility resolution from the TWIMS system is limited, leading to poor separation of isomers. In this respect, cyclic ion mobility mass spectrometer with its higher ion mobility resolution could be used to improve the separation of isomers from wood pyrolysis products. Also, the ion mobility analysis procedure and the data processing workflow could be used to differentiate a larger group of biomass species. Future studies will involve the analysis of more standard molecules, including lignin dimers, for the creation of a $^{TW}CCS_{N2}$ database for wood degradation products. Finally, the calculation of theoretical CCS could be foreseen with different

isomers from wood degradation products to confirm in-silico experimental CCS obtained with ASAP IMS TOF.

Acknowledgements

The COBRA laboratory is financed by the Labex SynOrg (ANR-11-LABX-0029) and the European Regional Development Fund (ERDF HN0001343). Financial support from the National Fourier transform ion cyclotron resonance network (FR 3624 CNRS) and the European Union's Horizon 2020 Research Infrastructures program (grant agreement 731077), are gratefully acknowledged.

Appendix and electronic component

Tables of the experimental parameters for the DIP APCI FTICR MS and the ASAP IM TOF MS analyses of biomass pellets and CCS calibrants; list of ions used for internal calibration of DIP FTICR spectra; PAH mix used for CCS calibration; list of standard molecules putatively identified in the wood pyrolysis process; list of notable ions observed the pyrolysis of biomass pellets, including putative structures and relative mass errors observed with FTICR and TOF MS; molecular formulas extracted from the PCA on ASAP TOF MS; tables of $^{TW}CCS_{N2}$ (calibrated with PAHs or polyalanine) of sixty molecular markers obtained from the pyrolysis of biomass samples; mass spectra of beech pyrolysis; Venn diagrams on lists of molecular formulas; MS/MS spectra. Excel file with all attributions, absolute and normalized intensities.

References

1. (IEA), I.E.A., *Bioenergy Power Generation* 2020.
2. Reichstein, M., et al., *Climate extremes and the carbon cycle.* Nature, 2013. **500**(7462): p. 287-295.
3. SjÖStrÖM, E., *Chapter 1 - THE STRUCTURE OF WOOD*, in *Wood Chemistry (Second Edition)*, E. SjÖStrÖM, Editor. 1993, Academic Press: San Diego. p. 1-20.
4. Pettersen, R.C., *The Chemical Composition of Wood*, in *The Chemistry of Solid Wood*. 1984, American Chemical Society. p. 57-126.
5. Poletto, M., A.J. Zattera, and R.M.C. Santana, *Structural differences between wood species: Evidence from chemical composition, FTIR spectroscopy, and thermogravimetric analysis.* J. Appl. Polym. Sci., 2012. **126**(S1): p. E337-E344.
6. Boerjan, W., J. Ralph, and M. Baucher, *Lignin Biosynthesis.* Annu. Rev. Plant Biol, 2003. **54**(1): p. 519-546.
7. Basu, P., *Chapter 5 - Pyrolysis*, in *Biomass Gasification, Pyrolysis and Torrefaction (Third Edition)*, P. Basu, Editor. 2018, Academic Press. p. 155-187.
8. Balat, M., *Mechanisms of Thermochemical Biomass Conversion Processes. Part 1: Reactions of Pyrolysis.* Energy Sources, Part A: Recovery, Utilization, and Environmental Effects, 2008. **30**(7): p. 620-635.
9. Dhyani, V. and T. Bhaskar, *Chapter 9 - Pyrolysis of Biomass*, in *Biofuels: Alternative Feedstocks and Conversion Processes for the Production of Liquid and Gaseous Biofuels (Second Edition)*, A. Pandey, et al., Editors. 2019, Academic Press. p. 217-244.
10. Maschio, G., C. Koufopanos, and A. Lucchesi, *Pyrolysis, a promising route for biomass utilization.* Bioresour. Technol., 1992. **42**(3): p. 219-231.
11. Dworzanski, J.P. and H.L.C. Meuzelaar, *Pyrolysis Mass Spectrometry, Methods ☆*, in *Encyclopedia of Spectroscopy and Spectrometry (Third Edition)*, J.C. Lindon, G.E. Tranter, and D.W. Koppenaal, Editors. 2017, Academic Press: Oxford. p. 789-801.
12. Stout, S.A., J.J. Boon, and W. Spackman, *Molecular aspects of the peatification and early coalification of angiosperm and gymnosperm woods.* Geochim. Cosmochim. Acta, 1988. **52**(2): p. 405-414.
13. Pouwels, A.D. and J.J. Boon, *Analysis of beech wood samples, its milled wood lignin and polysaccharide fractions by curie-point and platinum filament pyrolysis-mass spectrometry.* J. Anal. Appl. Pyrolysis, 1990. **17**(2): p. 97-126.
14. van der Hage, E.R.E., M.M. Mulder, and J.J. Boon, *Structural characterization of lignin polymers by temperature-resolved in-source pyrolysis—mass spectrometry and Curie-point pyrolysis—gas chromatography/mass spectrometry.* J. Anal. Appl. Pyrolysis, 1993. **25**: p. 149-183.
15. Christensen, E., R.J. Evans, and D. Carpenter, *High-resolution mass spectrometric analysis of biomass pyrolysis vapors.* J. Anal. Appl. Pyrolysis, 2017. **124**: p. 327-334.
16. Sobeih, K.L., M. Baron, and J. Gonzalez-Rodriguez, *Recent trends and developments in pyrolysis-gas chromatography.* J Chromatogr A, 2008. **1186**(1-2): p. 51-66.
17. Morgan, T.J. and R. Kandiyoti, *Pyrolysis of coals and biomass: analysis of thermal breakdown and its products.* Chem Rev, 2014. **114**(3): p. 1547-607.
18. Kumagai, S., et al., *Combining pyrolysis–two-dimensional gas chromatography–time-of-flight mass spectrometry with hierarchical cluster analysis for rapid identification of pyrolytic interactions: Case study of co-pyrolysis of PVC and biomass components.* Process. Saf. Environ. Prot., 2020. **143**: p. 91-100.
19. McEwen, C.N., R.G. McKay, and B.S. Larsen, *Analysis of Solids, Liquids, and Biological Tissues Using Solids Probe Introduction at Atmospheric Pressure on Commercial LC/MS Instruments.* Anal. Chem., 2005. **77**(23): p. 7826-7831.

20. Barrère, C., et al., *Rapid analysis of polyester and polyethylene blends by ion mobility-mass spectrometry.* Polym. Chem., 2014. **5**(11): p. 3576-3582.
21. Fan, X., et al., *Rapid characterization of heteroatomic molecules in a bio-oil from pyrolysis of rice husk using atmospheric solids analysis probe mass spectrometry.* J. Anal. Appl. Pyrolysis, 2015. **115**: p. 16-23.
22. Bruns, E.A., et al., *Atmospheric Solids Analysis Probe Mass Spectrometry: A New Approach for Airborne Particle Analysis.* Anal. Chem., 2010. **82**(14): p. 5922-5927.
23. Farenc, M., et al., *Characterization of Polyolefin Pyrolysis Species Produced Under Ambient Conditions by Fourier Transform Ion Cyclotron Resonance Mass Spectrometry and Ion Mobility-Mass Spectrometry.* J. Am. Soc. Mass. Spectrom., 2017. **28**(3): p. 507-514.
24. Aubriet, F., et al., *Characterization of biomass and biochar by LDI-FTICRMS – Effect of the laser wavelength and biomass material.* J. Am. Soc. Mass. Spectrom., 2018. **29**(10): p. 1951-1962.
25. Abdelnur, P.V., et al., *Characterization of Bio-oils from Different Pyrolysis Process Steps and Biomass Using High-Resolution Mass Spectrometry.* Energy Fuels, 2013. **27**(11): p. 6646-6654.
26. Rüger, C.P., et al., *Characterisation of ship diesel primary particulate matter at the molecular level by means of ultra-high-resolution mass spectrometry coupled to laser desorption ionisation—comparison of feed fuel, filter extracts and direct particle measurements.* Anal. Bioanal. Chem. 2015. **407**(20): p. 5923-5937.
27. Kanu, A.B., et al., *Ion mobility–mass spectrometry.* J. Mass Spectrom., 2008. **43**(1): p. 1-22.
28. Barrère, C., et al., *Atmospheric Solid Analysis Probe–Ion Mobility Mass Spectrometry of Polypropylene.* Anal. Chem., 2012. **84**(21): p. 9349-9354.
29. Vieillard, J., et al., *Atmospheric Solid Analysis Probe-Ion Mobility Mass Spectrometry: An Original Approach to Characterize Grafting on Cyclic Olefin Copolymer Surfaces.* Langmuir, 2015. **31**(48): p. 13138-13144.
30. Lawrence, A.H., R.J. Barbour, and R. Sutcliffe, *Identification of wood species by ion mobility spectrometry.* Anal. Chem., 1991. **63**(13): p. 1217-1221.
31. Roger, C.P., C.W. James, and H.L. André, *Detection of Northern Red Oak Wetwood by Fast Heating and Ion Mobility Spectrometric Analysis.* Holzforschung, 1993. **47**(6): p. 513-522.
32. Castilla, C., et al., *Direct Inlet Probe Atmospheric Pressure Photo and Chemical Ionization Coupled to Ultrahigh Resolution Mass Spectrometry for the Description of Lignocellulosic Biomass.* J. Am. Soc. Mass. Spectrom., 2020. **31**(4): p. 822-831.
33. Smith, D.P., et al., *Deciphering Drift Time Measurements from Travelling Wave Ion Mobility Spectrometry-Mass Spectrometry Studies.* Eur. J. Mass Spectrom., 2009. **15**(2): p. 113-130.
34. Bush, M.F., I.D.G. Campuzano, and C.V. Robinson, *Ion Mobility Mass Spectrometry of Peptide Ions: Effects of Drift Gas and Calibration Strategies.* Anal. Chem., 2012. **84**(16): p. 7124-7130.
35. Zheng, X., et al., *Utilizing ion mobility spectrometry and mass spectrometry for the analysis of polycyclic aromatic hydrocarbons, polychlorinated biphenyls, polybrominated diphenyl ethers and their metabolites.* Anal. Chim. Acta, 2018. **1037**: p. 265-273.
36. Deschamps, E., et al., *Determination of the collision cross sections of cardiolipins and phospholipids from Pseudomonas aeruginosa by traveling wave ion mobility spectrometry-mass spectrometry using a novel correction strategy.* Anal. Bioanal. Chem., 2019. **411**(30): p. 8123-8131.
37. van den Berg, R.A., et al., *Centering, scaling, and transformations: improving the biological information content of metabolomics data.* BMC Genomics, 2006. **7**(1): p. 142.
38. Haynes, S.E., et al., *Variable-Velocity Traveling-Wave Ion Mobility Separation Enhancing Peak Capacity for Data-Independent Acquisition Proteomics.* Anal. Chem., 2017. **89**(11): p. 5669-5672.
39. Wang, S., et al., *Mechanism research on cellulose pyrolysis by Py-GC/MS and subsequent density functional theory studies.* Bioresource Technology, 2012. **104**: p. 722-728.
40. Amen-Chen, C., H. Pakdel, and C. Roy, *Production of monomeric phenols by thermochemical conversion of biomass: a review.* Bioresour. Technol., 2001. **79**(3): p. 277-299.

41. Kim, S., R.W. Kramer, and P.G. Hatcher, *Graphical Method for Analysis of Ultrahigh-Resolution Broadband Mass Spectra of Natural Organic Matter, the Van Krevelen Diagram.* Anal. Chem., 2003. **75**(20): p. 5336-5344.
42. Simoneit, B.R.T., et al., *Molecular characterization of smoke from campfire burning of pine wood (Pinus elliottii).* Chemosphere, 2000. **2**(1): p. 107-122.
43. Rüger, C.P., et al., *Hyphenation of Thermal Analysis to Ultrahigh-Resolution Mass Spectrometry (Fourier Transform Ion Cyclotron Resonance Mass Spectrometry) Using Atmospheric Pressure Chemical Ionization For Studying Composition and Thermal Degradation of Complex Materials.* Anal. Chem., 2015. **87**(13): p. 6493-6499.
44. Choi, J.W., O. Faix, and D. Meier, *Characterization of Residual Lignins from Chemical Pulps of Spruce (Picea abies L.) and Beech (Fagus sylvatica L.) by Analytical Pyrolysis–Gas Chromatography/Mass Spectrometry.* Holzforschung, 2001. **55**(2): p. 185-192.
45. Gabelica, V., et al., *Recommendations for reporting ion mobility Mass Spectrometry measurements.* Mass Spectrom. Rev., 2019. **38**(3): p. 291-320.
46. Schauer, J.J., et al., *Measurement of Emissions from Air Pollution Sources. 3. C1−C29 Organic Compounds from Fireplace Combustion of Wood.* Environ. Sci. Technol., 2001. **35**(9): p. 1716-1728.
47. Sjöström, E., *Wood chemistry : fundamentals and applications*. 1993.
48. Farenc, M., et al., *Effective Ion Mobility Peak Width as a New Isomeric Descriptor for the Untargeted Analysis of Complex Mixtures Using Ion Mobility-Mass Spectrometry.* J. Am. Soc. Mass. Spectrom., 2017. **28**(11): p. 2476-2482.

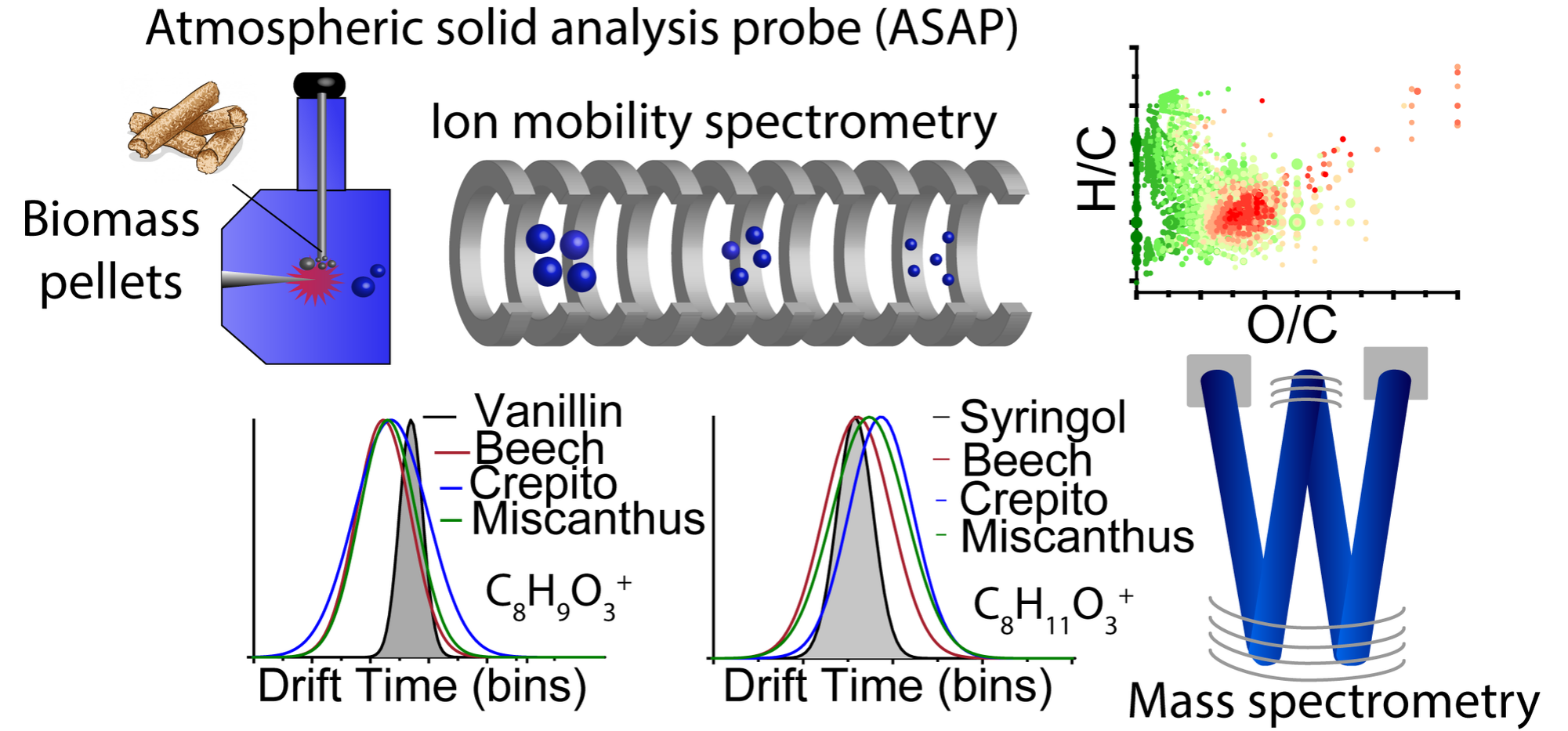
Atmospheric solid analysis probe (ASAP)
Biomass pellets
Ion mobility spectrometry
H/C
O/C
Vanillin
Beech
Crepito
Miscanthus
$C_8H_9O_3^+$
Drift Time (bins)
Syringol
Beech
Crepito
Miscanthus
$C_8H_{11}O_3^+$
Drift Time (bins)
Mass spectrometry